Drug Design, Development and Therapy Dovepress

Open Access Full Text Article ORIGINAL RESEARCH

Alkannin Induces G2/M-Phase Arrest, Apoptosis, and Inhibition of Invasion by Targeting GSK3β in Esophageal Squamous Cell Carcinoma

Huihui Ma[1–3,*], Peng Xu[1–3,*], Yunchao Jia[1,2], Yehan Zhou[1–3], Xinzhi Li[1,2,4], Yanming Wang[1–3], Ketao Ma[1–3]

[1]Key Laboratory of Xinjiang Endemic and Ethnic Diseases, Ministry of Education, Shihezi University School of Medicine, Shihezi, 832003, People's Republic of China; [2]NHC Key Laboratory of Prevention and Treatment of Central Asia High Incidence Diseases, First Affiliated Hospital, Shihezi University School of Medicine, Shihezi, 832003, People's Republic of China; [3]Department of Physiology, Shihezi University School of Medicine, Shihezi, 832003, People's Republic of China; [4]Department of Pathophysiology, Shihezi University School of Medicine, Shihezi, 832003, People's Republic of China

*These authors contributed equally to this work

Correspondence: Ketao Ma; Yanming Wang, Department of Physiology, Shihezi University School of Medicine, Shihezi, 832003, People's Republic of China, Tel +86 150 0164 5180; +86 175 9093 3308, Email maketao@hotmail.com; wangyanminglyo@163.com

Purpose: Esophageal squamous cell carcinoma (ESCC) is the most common malignant tumor of the upper gastrointestinal tract, characterized by high mortality and poor prognosis. There is an urgent need for the development of more effective drugs. Alkannin has been shown to inhibit the progression of various cancers, but its inhibitory effects on ESCC remain unclear. This study aims to investigate the therapeutic effects of Alkannin on ESCC and elucidate its potential targets and molecular mechanisms.

Methods: Cell Counting Kit-8 (CCK-8) assays, colony formation assays, Hoechst 33342 staining, wound healing assays, Transwell migration assays, flow cytometry, and Western blotting were used to investigate the therapeutic effects of Alkannin on ESCC in vitro. Transcriptome sequencing and network pharmacology were employed to analyze the potential targets and pathways affected by Alkannin treatment. The anticancer effects of Alkannin in vivo were assessed in a nude mouse model.

Results: Alkannin suppressed cell proliferation, invasion, migration, and induced ESCC cell apoptosis. Mechanistic studies indicated that Alkannin inhibits ESCC by inducing G2/M-phase cell cycle arrest by targeting Glycogen Synthase Kinase 3β (GSK3β). Consistently, in vivo administration of Alkannin significantly reduced the growth of ESCC tumors in nude mice.

Conclusion: This study is the first to demonstrate that Alkannin, by targeting GSK3β, induces G2/M-phase arrest in ESCC cells, thereby inhibiting migration, invasion, and inducing apoptosis, suggesting that Alkannin may be a promising antitumor agent for treating ESCC.

Keywords: esophageal squamous cell carcinoma, Alkannin, network pharmacology, transcriptomics, Glycogen Synthase Kinase 3β

Introduction

Esophageal cancer has a high incidence and mortality rate worldwide. According to 2020 GLOBOCAN cancer statistics, an estimated 604,000 new cases of esophageal cancer were diagnosed globally, with approximately 544,000 deaths.[1,2] Notably, around 55% of esophageal cancer cases occur in China, with esophageal squamous cell carcinoma (ESCC) accounting for over 90% of these cases.[3,4] Despite the various treatment strategies for ESCC in clinical practice, their efficacy remains limited and unsatisfactory. Consequently, there is an urgent need to explore new and more effective therapeutic approaches.[5,6]

Glycogen Synthase Kinase 3β (GSK3β) is a ubiquitously expressed serine/threonine kinase involved in tumorigenesis. GSK3β expression is elevated in various cancers, such as melanoma, pancreatic cancer, ovarian cancer, and prostate cancer.[7] Aberrant GSK3β expression is associated with multiple malignant phenotypes of cancers, including migration, invasion, apoptosis, and cell cycle dysregulation.[8] Studies have shown that genetic suppression and pharmacological

Received: 17 June 2024
Accepted: 9 November 2024
Published: 25 November 2024

Graphical Abstract

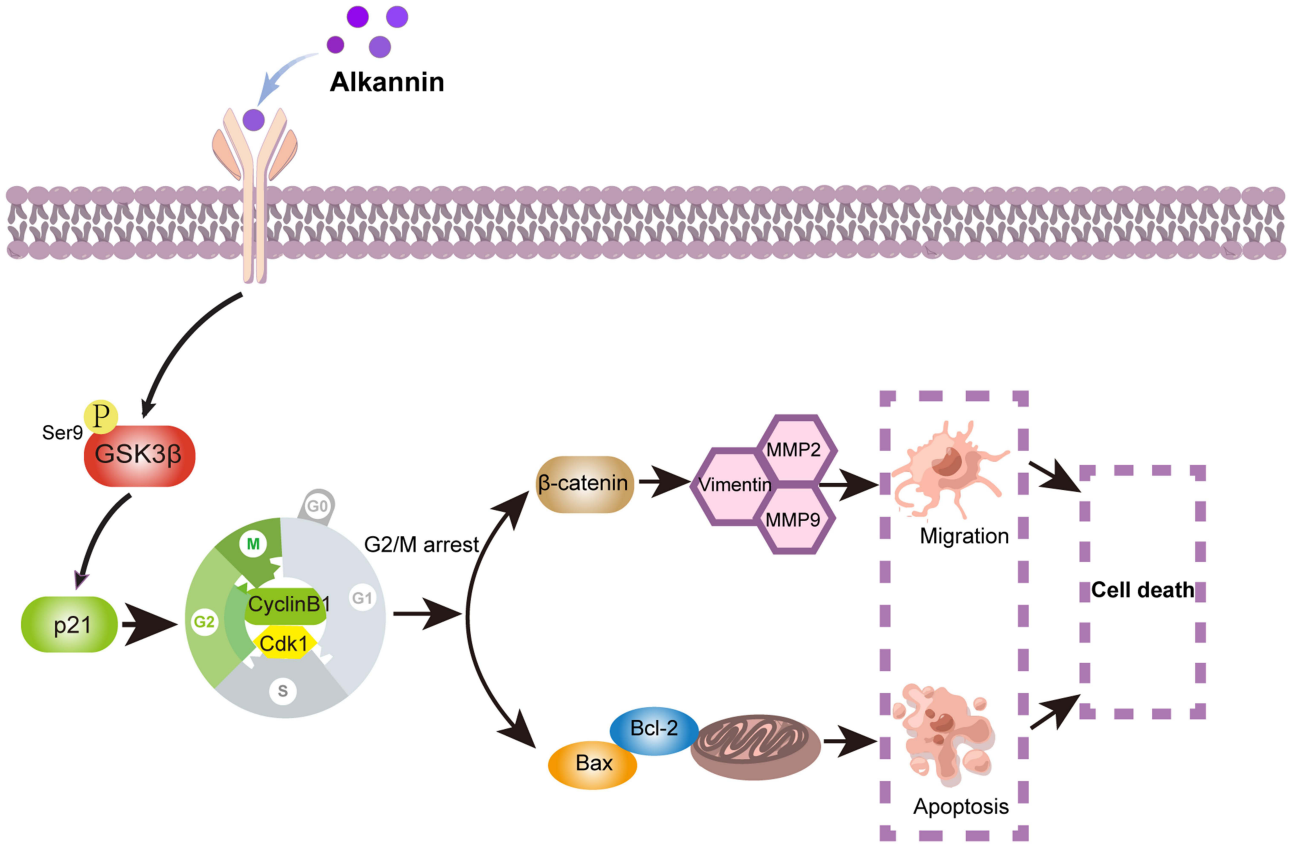

inhibition of GSK3β increase apoptosis-related protein levels and induce tumor cell apoptosis.[9] Additionally, a reduction in GSK3β activity inhibits tumor cell migration and invasion by suppressing the epithelial–mesenchymal transition (EMT).[10,11] Recent studies have indicated that GSK3β expression and activity in ESCC cell lines and primary tumors are higher than those in normal esophageal squamous mucosal cells and tissues. GSK3β inhibition reduced tumor cell survival and proliferation, inducing apoptosis in ESCC cells and xenograft tumors.[12] Research shows that inhibiting GSK3β activity effectively curbs the growth of esophageal and other cancers. Therefore, developing GSK3β inhibitors may be a key research direction for future cancer treatments.

Alkannin is one of the chief active components of *Lithospermum erythrorhizon*. It exhibits therapeutic properties, including anti-inflammatory, antibacterial, antitumor, and antioxidant activities.[13] Recent studies have highlighted the potent anticancer effects of Alkannin. It promotes apoptosis in skin squamous cell carcinoma cells by enhancing PTEN expression and M1 macrophage polarization, thus impeding carcinoma progression.[14] It also modulates the microRNA-9/RECK axis, suppressing the growth, migration, and invasion of oral squamous carcinoma cells.[15] Moreover, Alkannin might also be a novel compound for treating glioma cells through cell cycle arrest, the induction of apoptosis, and the blockage of cell migration and invasion.[16,17] However, the antitumor effect of Alkannin in ESCC and its specific targeted signaling pathways have not been investigated.

Materials and Methods

Materials

Alkannin was obtained from MCE (purity ≥ 99%, HY-N6012). Specific antibodies, including anti-PCNA (1:1000, ab29), anti-Bax (1:1000, ab32503), anti-Bcl-2 (1:1000, ab32124), and anti-p21 (1:1000, ab109520), were obtained from Abcam.

Other antibodies, such as anti-MMP2 (1:1000, BM4075), anti-Ki67 (1:1000, A00254), and anti-CyclinB1 (1:1000, BM4370), were obtained from Boster Biological Technology Co., Ltd. (Shanghai, China). Anti-CDK1 (1:1000, 19,532-1-IG) and anti-vimentin (1:1000, 10,366-1-AP) were obtained from Proteintech Group, Inc. (Wuhan, China). Anti-MMP9 (1:1000, bsm-54040R) was acquired from Bioss Biotechnology Co., Ltd. (Beijing, China). Other antibodies, including against GSK3β (1:1000, #9315s), p-GSK3β (1:1000, #9323s), and β-catenin (1:1000, #8480s), were purchased from CST. A Cell Counting Kit 8 (CCK-8) detection kit was obtained from APExBIO Technology LLC (Shanghai, China). Both the Annexin V-FITC/PI and cell cycle kits were obtained from MultiSciences (Lianke) Biotechnology Corporation Limited (Hangzhou, China). Fetal bovine serum (FBS) was obtained from BI (Israel), and RPMI 1640 was obtained from Gibco (Grand Island, USA).

Cell Culture and Alkannin Treatment

The human ESCC cell lines KYSE150 and Eca109 (Procell Biosciences, Shanghai, China) were cultured in RPMI 1640 medium (Gibco, United States) supplemented with 10% fetal bovine serum (BI, Israel), 100 U/mL penicillin, and 100 μg/mL streptomycin (HyClone, United States). The cells were maintained in a humidified incubator (Thermo Fisher, United States) at 37°C with 5% CO_2. The 5 mg Alkannin powder (molecular weight: 288.30 g/mol) was dissolved in 1.73 mL of dimethyl sulfoxide (DMSO) to make the 10 mM stock solution, and the cell culture medium was used to dilute the stock solution to 0 μM, 2 μM, 4 μM and 6 μM in the cell treatment group.

Cell Counting Kit-8 Assay

KYSE150 (5×10^3/well) and Eca109 (8×10^3/well) cells were seeded into 96-well plates. After cell adherence, the cells were treated with various concentrations of Alkannin (0, 2, 4, 6, 8, and 10 μM) for 24, 48, and 72 hours. Post-treatment, 10 μL of CCK-8 solution was added to each well, and the plates were incubated for 1–2 hours protected from light. The absorbance (OD value) at 450 nm was measured using a microplate reader (Thermo Fisher). Cell viability was calculated using the following formula: Cell Viability (%) = (OD of the treatment group / OD of the control group) × 100.

Colony Formation Assay

KYSE150 and Eca109 cells (1×10^3/well) were seeded in 6-well plates and treated with different concentrations of Alkannin (0, 0.2, 0.4, 0.6 μM) for 24 hours. The medium containing Alkannin was removed, and the cells were cultured normally for 10 days. The cells were fixed with 4% paraformaldehyde, stained with 0.1% crystal violet solution, rinsed with distilled water, and photographed to count the colonies.

Wound Healing Assay

KYSE150 and Eca109 cells were cultured in 6-well plates until they reached 90% confluency. A pipette tip was used to create a scratch across the cell monolayer. The cells were gently washed three times with PBS and treated with Alkannin at concentrations of 0, 2, 4, and 6 μM. The scratch area was monitored and photographed at 0 hours and again at 24 hours under a microscope. Images of the scratch were analyzed using ImageJ. Cell migration was calculated according to the following formula: Cell migration ratio (%) = 100 × (0 h scratch width – 24 h scratch width) / 0 h scratch width.

Transwell Assay

The cell invasion experiment was conducted using Transwell chambers with 8 μm pore inserts (Corning, MA, USA). KYSE150 and Eca109 cells were resuspended in serum-free culture medium and counted. A total of 200 μL of the cell suspension (2×10^4 cells/well) was added to the upper chamber. The lower chamber was filled with 700 μL of complete culture medium containing various concentrations of Alkannin (0, 2, 4, and 6 μM) and 20% FBS. The chambers were incubated at 37°C with 5% CO_2 for 24 hours. After incubation, the cells that had invaded through the membrane were fixed with 4% paraformaldehyde for 30 minutes, stained with 0.1% crystal violet, and then photographed and counted.

Hoechst 33342 Staining Assay

KYSE150 and Eca109 cells were seeded in 6-well plates and cultured. After treatment with different concentrations of Alkannin for 24 hours, the cells were washed twice with PBS, fixed with 4% paraformaldehyde for 15 minutes, and stained with a diluted Hoechst 33342 solution for 10 minutes. The cells were washed twice with PBS to remove excess stain. Observations and imaging were conducted under a fluorescence microscope.

Annexin V-FITC/PI Apoptosis Assay

Cell apoptosis was assessed using an Annexin V-FITC/PI apoptosis kit. After 24 hours of treatment with Alkannin, the cells were trypsinised and washed with cold PBS. The cells were then resuspended in 500 μL of 1× binding buffer, stained with 5 μL of FITC Annexin V and 10 μL of PI (propidium iodide) solution, and incubated for 10 minutes at room temperature in the dark. The rate of apoptosis was determined using a FACSAria III flow cytometer (BD Biosciences).

Flow Cytometry Cell Cycle Assay

Cell cycle analysis was conducted using propidium iodide (PI) staining. After 24 hours of treatment with Alkannin, the cells were washed twice with cold PBS and then digested with trypsin to form a cell suspension. The cell suspension was added dropwise into cold absolute ethanol to ensure uniform mixing, followed by storage overnight at 4°C. Subsequently, the ethanol was removed, and 1 mL of DNA staining solution was added to the cells. The mixture was vortexed briefly and then incubated at 37°C in the dark for 30 minutes. Finally, the distribution of cells in different cell cycle phases (G0/G1, S, and G2/M) was analyzed using flow cytometry, and data analysis was conducted using ModFit software.

Western Blot Assay

Treated cells were lysed using ice-cold RIPA buffer supplemented with 1% phenylmethanesulfonyl fluoride (PMSF) for 30 minutes at 4°C. Proteins extracted from the lysates were quantified using a BCA protein assay kit (Thermo Fisher). After denaturation at high temperatures, 30–50 μg of protein samples were subjected to 10% SDS-PAGE and transferred onto PVDF membranes (Merck Millipore, United States). The membranes were blocked in 5% non-fat milk in TBST for 2–3 hours and incubated with primary antibodies (β-actin, PCNA, MMP2, MMP9, β-catenin, Vimentin, Bcl-2, Bax, CyclinB1, CDK1, GSK3β, p-GSK3β, p21; 1:1000 dilution) overnight at 4°C. After three 10-minute washes with TBST at room temperature, the membranes were treated with horseradish peroxidase-conjugated secondary antibodies (goat anti-rabbit or anti-mouse IgG) for 2 hours. The protein bands were visualized via enhanced chemiluminescence (ECL) with a Tanon 5200 system and quantitatively analyzed using ImageJ software.

RNA Extraction and Sequencing Analysis

KYSE150 cells were divided into two groups: a control group and a group treated with 4 μM Alkannin for 24 hours. RNA was extracted from KYSE150 cells using TRIzol reagent. The samples were examined using the Agilent 2200 System, and after passing quality control, RNA-seq transcriptome sequencing was conducted on the Illumina HiSeq high-throughput sequencing platform (NovelBio Company, Shanghai, China). Differentially expressed genes were annotated using the Gene Ontology (GO) framework. The Kyoto Encyclopedia of Genes and Genomes (KEGG) database was used to classify these genes into significantly enriched pathways.

Network Pharmacology

Potential target proteins of the ingredients in Alkannin were identified using the cyber tools PharmMapper (http://lilab-ecust.cn/pharmmapper/) and SuperPred (https://prediction.charite.de/). Information on esophageal squamous cell carcinoma (ESCC)-related targets was collected from GeneCards (https://www.genecards.org/). The common targets of Alkannin and ESCC were imported into the Metascape database (https://Metascape.org/) for GO annotation and KEGG enrichment analysis. Furthermore, in combination with the transcriptomic data, further KEGG pathway analysis was conducted to predict the key targets and pathways involved in the effect of Alkannin on ESCC treatment.

Molecular Docking

Molecular docking was performed to analyze the interaction between Alkannin and its key target. The SDF structure of Alkannin was downloaded from the PubChem database (https://pubchem.ncbi.nlm.nih.gov/), and the key target protein structure was obtained from the Protein Data Bank (PDB) database (https://www.rcsb.org/). It is reported that some promising therapeutic GSK3β inhibitors were found to inhibit GSK3β by binding to the ATP site, and most of the hydrogen bonding interactions are conserved as in GSK3β structures deposited. 1Q5K protein contains the structure of ATP pocket, which is located at the interface of the β-strand and α-helical domains. Furthermore, 1Q5K was obtained together with the ATP-competitive inhibitor AR-A014418, which provides a more detailed hydrogen bonding interactions basis as the control group in the study.[18,19] Therefore, 1Q5K is used as the ideal GSK3β crystal 3D structure for analyzing the binding mode analysis with Alkannin. The structures were optimized in Discovery Studio 2019 (DS2019), including ligand removal, dehydration, and hydrogen addition. We used specific docking to finish this analysis. The grid box coordinates of the docking procedure were X = 23.9922, Y = 22.8271, Z = 8.88419. Molecular docking of the protein with the small molecule in DS2019 produced 3D and 2D interaction schematics. The binding affinity was assessed using -CDOCKER INTERACTION ENERGY and compared with that of a positive control.

Establishment of Xenograft Mice Model and Treatment with Alkannin

Female BALB/c-nu athymic mice, aged 5 weeks and weighing 14–17 g, were purchased from SPF Biotechnology Co., Ltd., Beijing, China (License: SCXK (Beijing) 2019–0010). All animal welfare and experimental procedures were conducted in accordance with the National Institutes of Health Guide for the Care and Use of Laboratory Animals (NIH Publication No. 8023, Revised 1978) and approved by the Animal Ethics Committee of Shihezi University School of Medicine. Mice were housed in a specific pathogen-free environment and provided with sterile water and food. KYSE150 cells (1.0×10^7 cells in 100 μL PBS) were subcutaneously injected into the left axillary region of 18 mice. When the tumors reached a volume of 60–100 mm^3, the mice were randomly divided into three groups: Model Group, Low-Dose (2 mg/kg/d), and High-Dose (4 mg/kg/d) with six mice in each group. In vivo experiments, the 20 mg Alkannin powder was dissolved in 1 mL of DMSO to make the 20 mg/mL stock solution. The stock solution was diluted with 0.9% NaCl to achieve the final doses of 2 mg/kg and 4 mg/kg for animal administration. The treatment groups were treated with 2 mg/kg or 4 mg/kg of Alkannin by intraperitoneal injection. The model group received an intraperitoneal injection of 0.9% NaCl containing the same amount of DMSO. Tumor size was measured every 3 days using calipers. The tumor volume was calculated as $V = 0.5\times L\times W^2$ (L = longest diameter, W = shortest diameter). After 14 consecutive days of treatment and an additional 2 days without treatment, mice were anesthetized with 40 mg/kg pentobarbital sodium. The tumors were then excised, measured, weighed, and documented through photographs.

Hematoxylin and Eosin (H&E) Staining

Tumor samples were fixed in 4% paraformaldehyde, embedded in paraffin, and transversely cut into 4 μm sections using a microtome. The sections were subjected to hematoxylin–eosin (H&E) staining and mounted using a neutral resin. Microscopic observations and imaging were then performed.

Immunohistochemical Staining

Paraffin-embedded tumor sections were deparaffinized in sequential xylene solutions and dehydrated in graded ethanol. Antigen retrieval was performed via a heat-induced method using EDTA solution, and endogenous peroxidase activity was blocked by incubating the sections in a 3% H_2O_2 solution. Primary antibodies against Ki67 and p-GSK3β (both at 1:100 dilution) were added and incubated overnight at 4°C. A universal secondary antibody was applied for 30 minutes at 37°C. After 3,3'-diaminobenzidine (DAB) staining, the nuclei were stained with haematoxylin. Then, images were obtained with a microscope.

Statistical Analysis

The data obtained in the study were processed using SPSS 26.0 software. One-way analysis of variance (ANOVA) was used to assess the differences between the experimental and control groups, and then Tukey's test was performed to analyse the differences between multiple groups according to the chi-square test. The statistical results are expressed as the mean ± standard deviation (SD). $P < 0.05$ was considered to indicate statistical significance. The statistical results were visualized using GraphPad Prism 9.0 software.

Results

Alkannin Inhibits the Proliferation of ESCC Cells

Cell proliferation was assessed using the CCK-8 assay, colony formation assays, and proliferating cell nuclear antigen (PCNA) protein expression analysis. The chemical structure of Alkannin is depicted in Figure 1A. KYSE150 and Eca109 cells were treated with varying concentrations (0, 2, 4, 6, 8, and 10 μM) of Alkannin for different periods of time (24 h, 48 h, or 72 h). Cell viability was evaluated using the CCK-8 assay. As shown in Figure 1B, Alkannin significantly reduced the viability of both KYSE150 and Eca109 cells in a concentration- and duration-dependent manner. Additionally, after Alkannin exposure for 24, 48, and 72 hours, the IC50 values for KYSE150 cells were 4.579 μM, 3.204 μM, and 2.449 μM, respectively. Similarly, the values for Eca109 cells were 3.8 μM, 3.589 μM, and 2.615 μM. Following 24 hours of Alkannin exposure at concentrations of 0.2, 0.4, and 0.6 μM, colony formation by KYSE150 and Eca109 cells decreased significantly (Figure 1C). Western blot analysis was used to measure the protein levels of PCNA, which is indicative of cell proliferation. The results showed a significant reduction in PCNA protein levels in both cell lines following Alkannin treatment (Figure 1D). In conclusion, Alkannin effectively inhibits the proliferation of ESCC cells.

Alkannin Suppresses Migration and Invasion in ESCC Cells

The aggressive invasiveness and metastatic potential of esophageal carcinoma present significant therapeutic challenges.[20] Consequently, scratch assays, Transwell chamber experiments, and protein expression analysis were employed to assess the migration and invasion capabilities of KYSE150 and Eca109 cells. After 24 hours of Alkannin treatment, the scratch assay results indicated concentration-dependent inhibition of cancer cell wound healing (Figure 2A). Transwell assays further confirmed the inhibitory effects of Alkannin on the migration and invasion of ESCC cells (Figure 2B). Key marker proteins, including matrix metalloproteinase-2 (MMP2), matrix metalloproteinase-9 (MMP9), Vimentin, and β-catenin, play pivotal roles in tumor migration and invasion.[21] Dose-dependent decreases in the protein levels of MMP2, MMP9, Vimentin, and β-catenin were revealed by Western blot analysis (Figure 2C). Collectively, these findings support the efficacy of Alkannin in suppressing the migration and invasion of ESCC cells.

Alkannin Induces Apoptosis in ESCC Cells

Cell apoptosis in KYSE150 and Eca109 cells was evaluated using Hoechst 33342 staining, Annexin V-FITC/PI double staining, and assessment of Bcl-2-associated X protein (Bax) and B-cell lymphoma-2 (Bcl-2) protein expression. After 24 hours of Alkannin treatment, Hoechst 33342 staining revealed a decrease in cell count and dense, chunk-like or fragmented nuclear staining compared to those in the control group (Figure 3A), suggesting that Alkannin might induce cell shrinkage and nuclear fragmentation to varying degrees. Annexin V-FITC/PI staining revealed that ESCC cells exhibited a dose-dependent increase in the proportion of both early and late apoptotic cells (Figure 3B). For the KYSE150 cells, the mean percentages of apoptotic cells (derived from five independent experiments) were 6.3% (2 μM), 12.7% (4 μM), and 23.1% (6 μM); similarly, for the Eca109 cells, the percentages were 7.3% (2 μM), 12.8% (4 μM), and 18.1% (6 μM). An increasing dose of Alkannin was associated with a significant increase in ESCC cell apoptosis. Furthermore, Western blot analysis confirmed an increase in the level of the proapoptotic protein Bax and a decrease in the level of the antiapoptotic protein Bcl-2 following treatment (Figure 3C). These results demonstrate that Alkannin induces apoptosis in ESCC cells in a concentration-dependent manner.

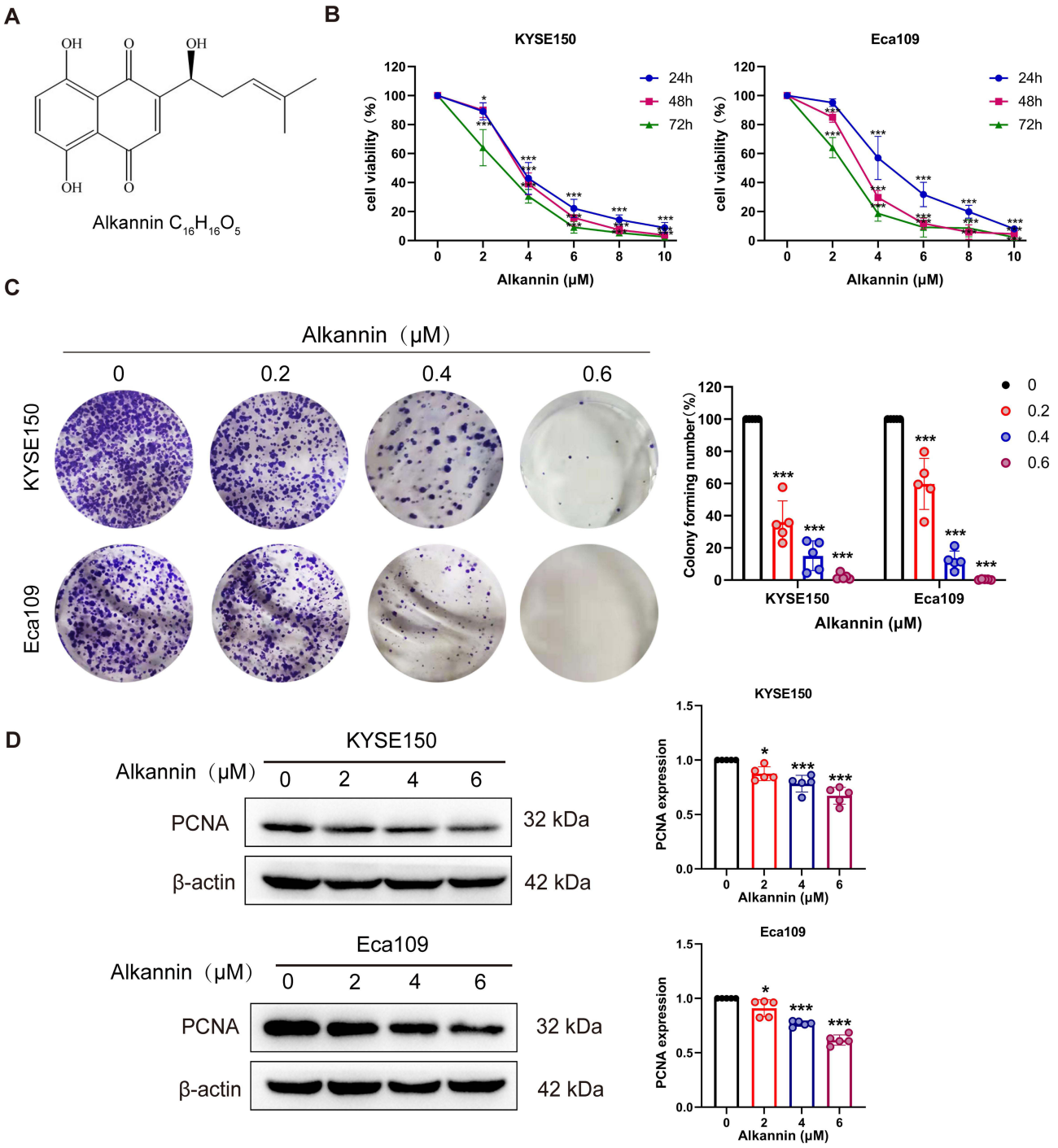

Figure 1 Alkannin inhibits the proliferation of ESCC cells. (**A**) Chemical structure of Alkannin. (**B**) Cell viability of KYSE150 and Eca109 cells treated with different concentrations of Alkannin for 24, 48, and 72 h. **(C)** Colony formation assay of KYSE150 and Eca109 cells after treatment with Alkannin for 24 h. **(D)** Western blot detects the PCNA protein levels of KYSE150 and Eca109 cells after treatment with Alkannin for 24 h. Data are expressed as means ± SD from five independent experiments, $^{*}P < 0.05$; $^{***}P < 0.001$ compared to control by one-way ANOVA.

Alkannin Induces G2/M Phase Arrest in ESCC Cells

To elucidate the mechanism underlying the inhibitory effect of Alkannin on ESCC proliferation, we used flow cytometry to analyze the impact of various Alkannin concentrations on the cell cycle distribution of ESCC cells. After 24 hours of Alkannin treatment, the percentages of KYSE150 cells in the G2/M phase (derived from five independent experiments) were 12.9% (0 μM), 15.1% (2 μM), 19.2% (4 μM), and 26.8% (6 μM). Similarly, the proportions of Eca109 cells were 8.9% (0 μM), 12.3%

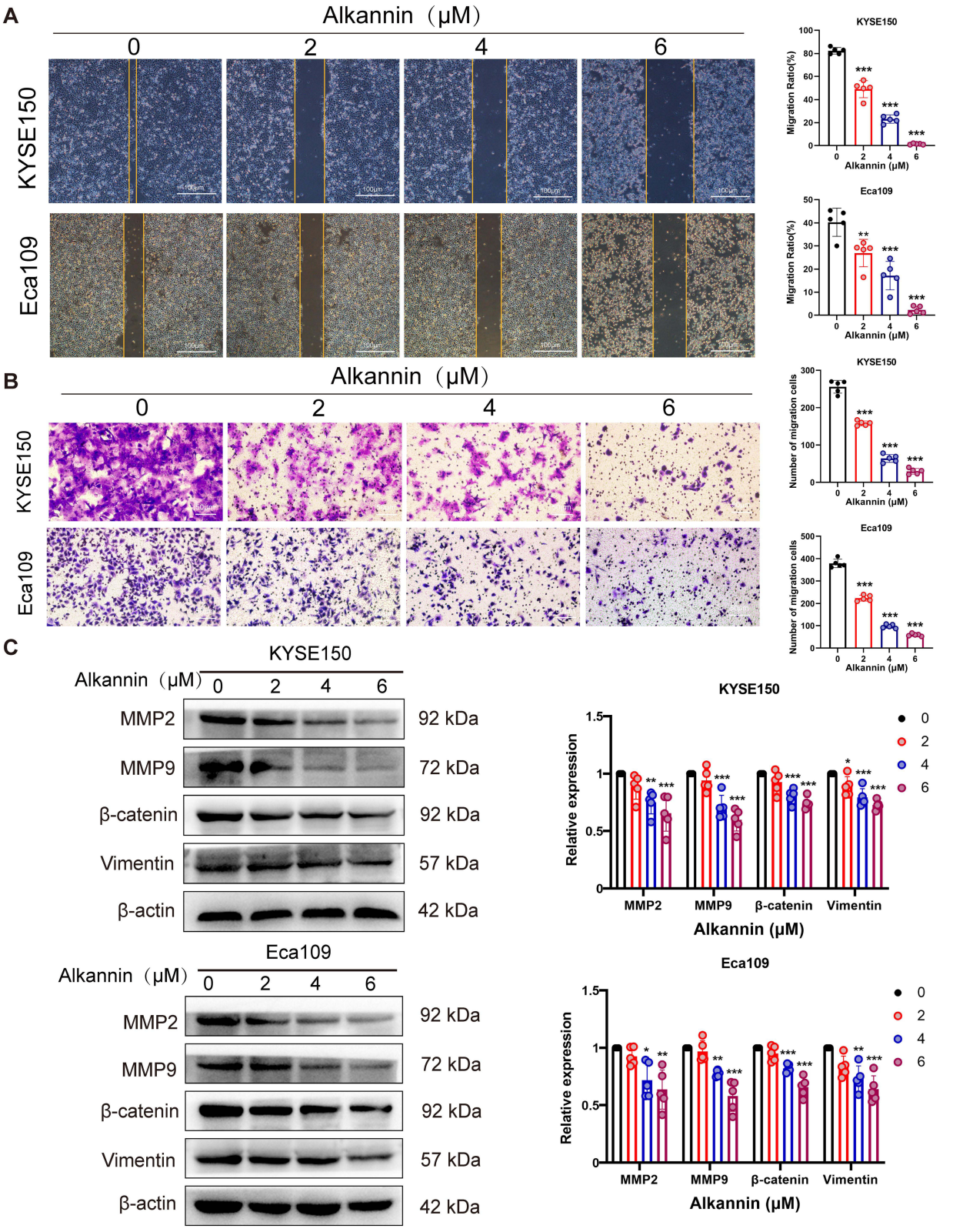

Figure 2 Alkannin inhibits the migration and invasion of ESCC cells. **(A)** Wound healing assay shows the mobility of KYSE150 and Eca109 cells after treatment with Alkannin. **(B)** Transwell assay detects the invasion ability of KYSE150 and Eca109 cells after treatment with Alkannin. **(C)** Western blot analyzes the protein expression of MMP2, MMP9, Vimentin, and β-Catenin in KYSE150 and Eca109 cells after treatment with Alkannin. Data are expressed as means ± SD from five independent experiments, **P* < 0.05; ***P* < 0.01; ****P* < 0.001 compared to control by one-way ANOVA.

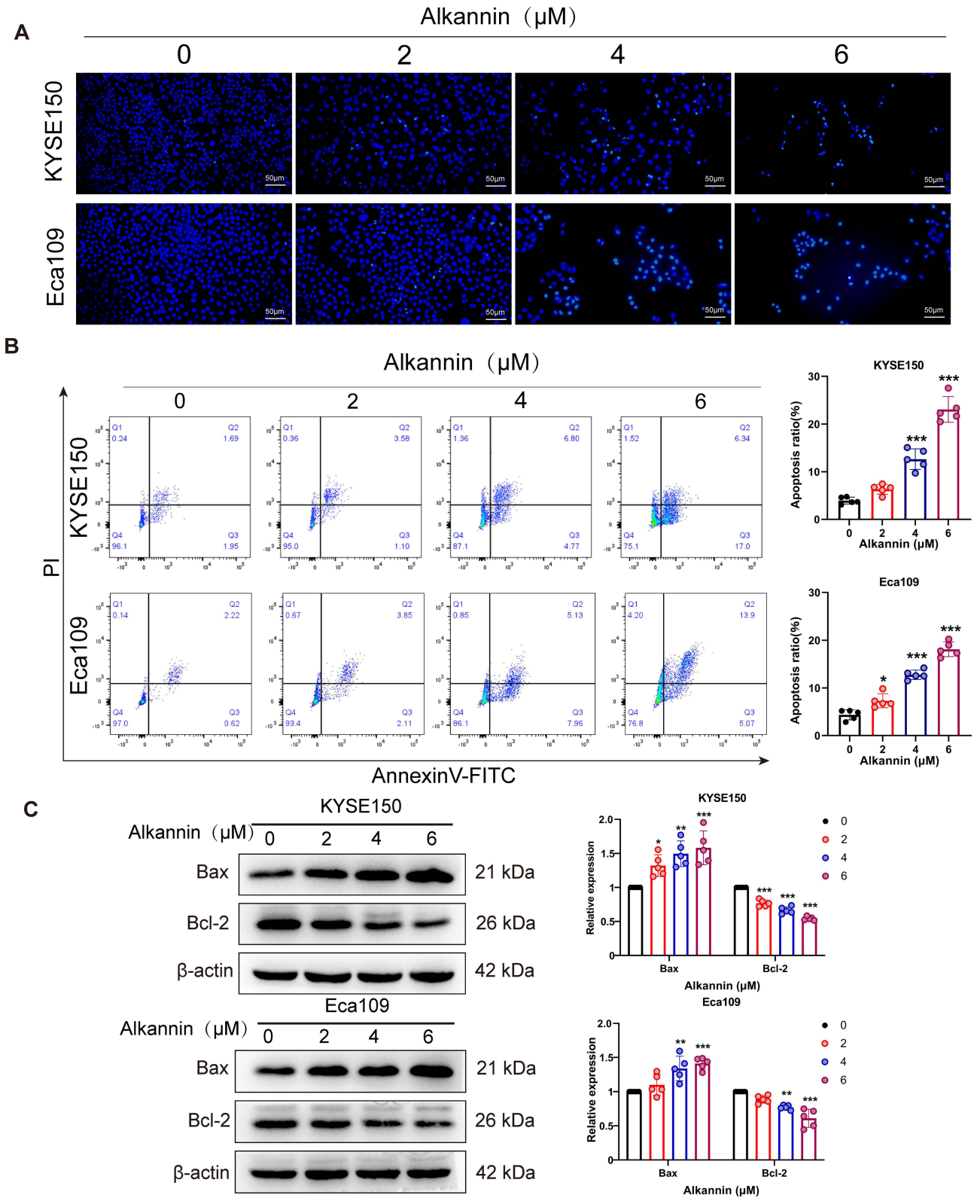

Figure 3 Alkannin induces apoptosis in ESCC cells. **(A)** Hoechst 33342 staining shows the extent of nuclear morphology of KYSE150 and Eca109 cells after treatment with different concentrations of Alkannin for 24 h. **(B)** Annexin V-FITC/PI assay is used to evaluate the apoptotic ratio of KYSE150 and Eca109 cells after treatment with Alkannin for 24 h. **(C)** Western blot analyzes the protein levels of BAX and Bcl-2 in KYSE150 and Eca109 cells. Data are expressed as means ± SD from five independent experiments, *$P < 0.05$; **$P < 0.01$; ***$P < 0.001$ compared to control by one-way ANOVA.

https://doi.org/10.2147/DDDT.S470061 DovePress

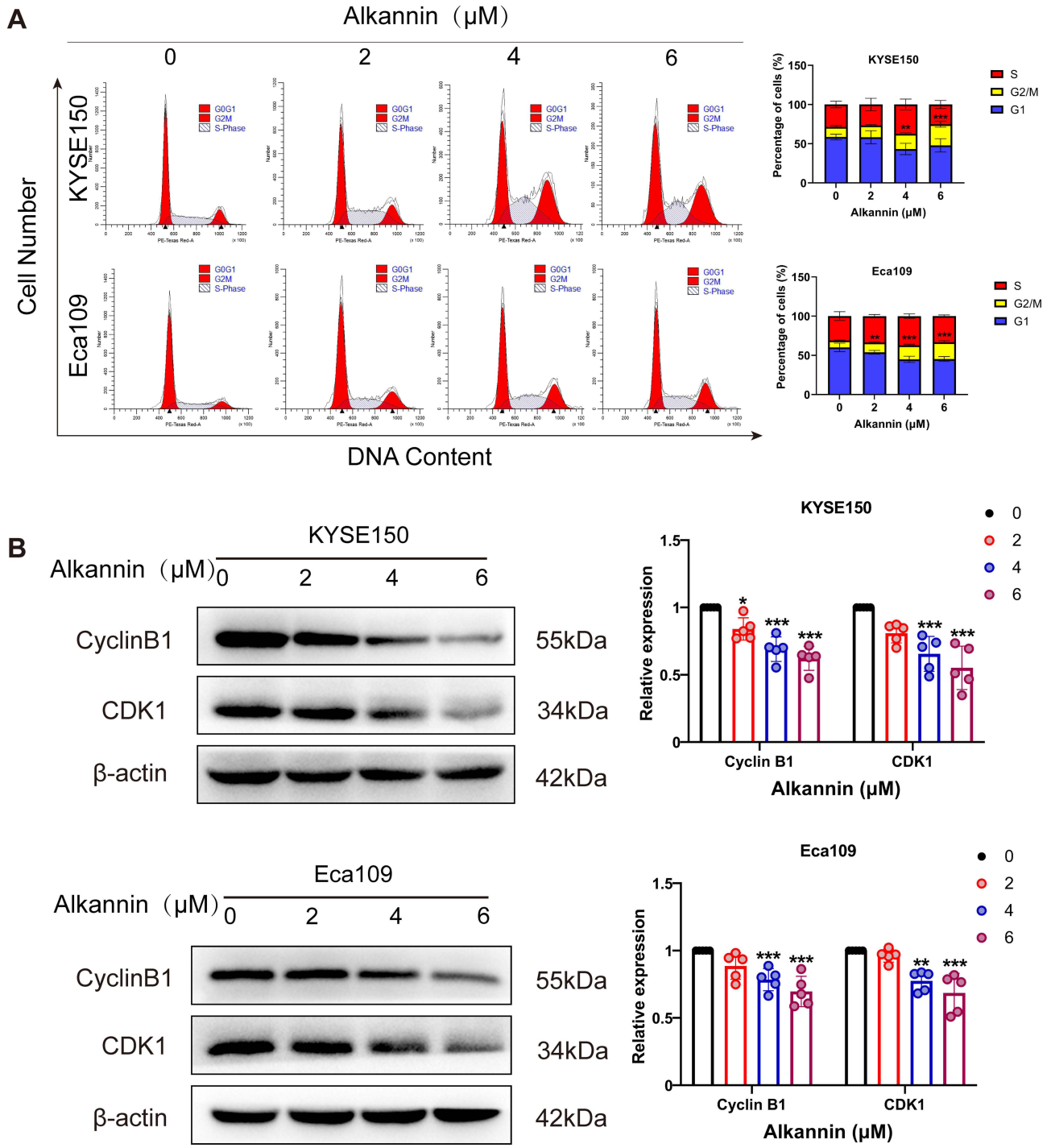

Figure 4 Alkannin induces G2/M phase arrest in ESCC cells. **(A)** Flow cytometry analysis shows cell cycle distribution of KYSE150 and Eca109 cells after treatment with Alkannin for 24 h. **(B)** Western blot analyzes the protein levels of CyclinB1 and CDK1 in KYSE150 and Eca109 cells after treatment with Alkannin for 24 h. Data are expressed as means ± SD from five independent experiments, $^{*}P < 0.05$; $^{**}P < 0.01$; $^{***}P < 0.001$ compared to control by one-way ANOVA.

(2 μM), 17.9% (4 μM), and 21.3% (6 μM). Alongside these findings, there was a notable decrease in the percentage of G1 phase cells, whereas the S phase cell population remained relatively stable (Figure 4A). Subsequently, the expression of G2/M phase-related proteins was examined using Western blotting. The results showed that Alkannin significantly reduced the levels of CyclinB1 and cyclin-dependent kinase 1 (CDK1) in ESCC cells (Figure 4B). Collectively, these data indicate that Alkannin effectively induces G2/M phase arrest in ESCC cells.

Transcriptomic Differential Gene Analysis Predicts the G2/M Phase as a Key Signaling Pathway

To gain a better understanding of the mechanistic effects of Alkannin on ESCC, transcriptomic sequencing of KYSE150 cells treated with Alkannin was performed. Compared to the control group, the Alkannin-treated group showed significant changes in gene expression, with 2534 genes upregulated and 2053 downregulated (Figure 5A and B). Enrichment analysis of these differentially expressed genes using GSEA highlighted the G2/M phase, which achieved an Enrichment Score (ES) of 0.5885 and a False Discovery Rate (FDR) of 0 (Figure 5C). Subsequent analysis using KEGG and GO enrichment methods on the downregulated genes further highlighted the cell cycle as a predominant feature in the outcomes. Importantly, the G2/M transition of the mitotic cell cycle occurred repeatedly within the top ten results of the GO enrichment analysis (Figure 5D and E). This finding corroborates our prior in vitro results, underscoring the G2/M phase of the cell cycle as a key factor in the efficacy of Alkannin against ESCC.

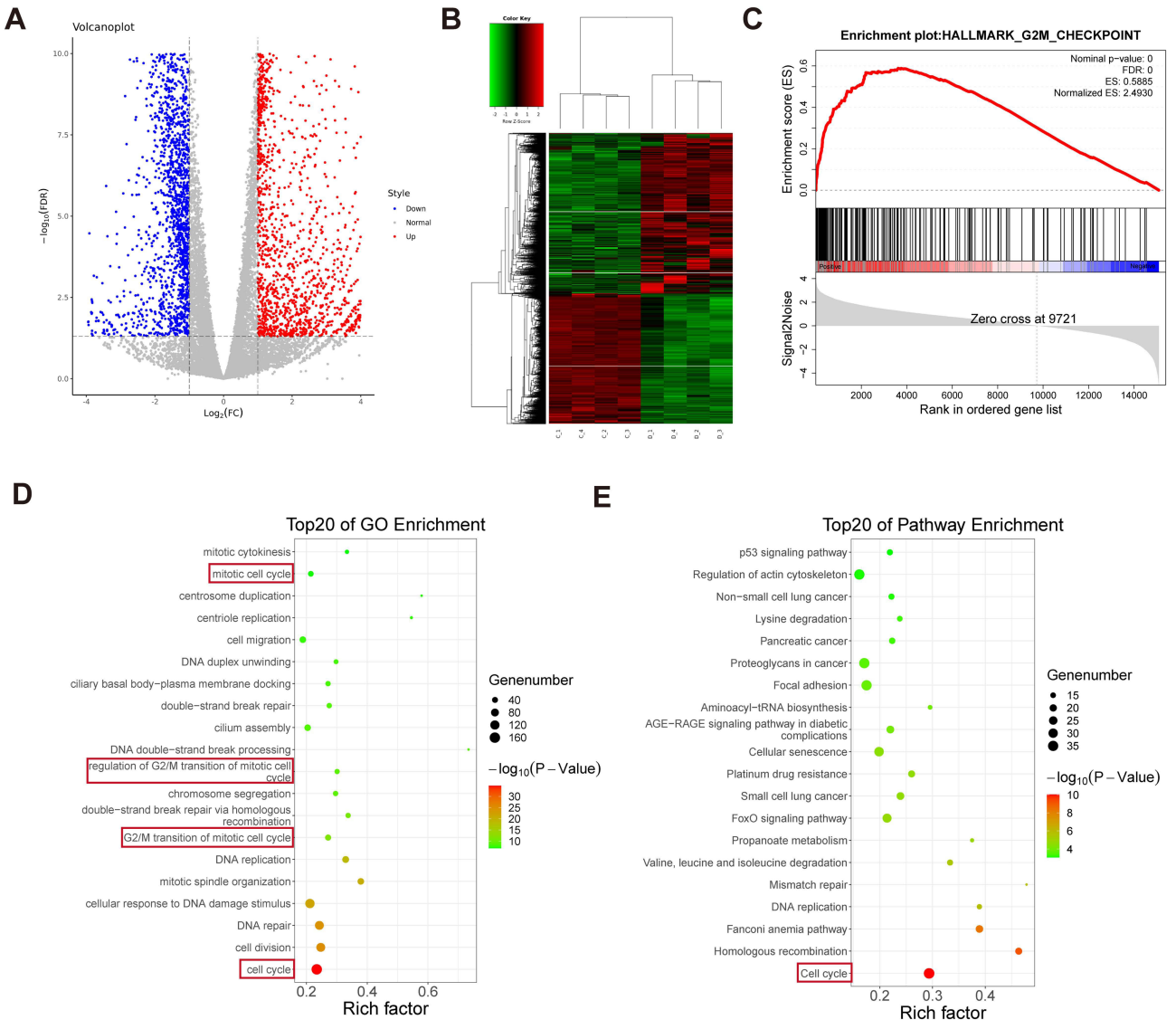

Figure 5 Transcriptomic analysis predicts the signal pathway of Alkannin anti-ESCC. **(A)** Volcano plot of differential gene expression (n = 4). Blue: downregulated, red: upregulated, gray: non-significant. **(B)** Heat map of differentially expressed genes. **(C)** Gene Set Enrichment Analysis (GSEA) map of the G2/M phase gene sets. **(D)** Gene Ontology (GO) enrichment analysis of pathways in the top 20. The red boxes indicate the most significantly enriched pathways for the G2/M phase and cell cycle that appear frequently. **(E)** KEGG enrichment analysis of the top 20 signaling pathways, with the red boxes highlighting the highest-ranked pathways and the cell cycle pathway ranked first.

Transcriptomic Analysis in Conjunction with Network Pharmacology Identifies GSK3β as the Key Target

Using drug target databases, PharmMapper and the Prediction Charite database, we identified 368 Alkannin-associated targets. Drawing from the disease target database GeneCards, a list of 4786 ESCC-related targets was assembled. A comparative analysis between these databases revealed 239 common targets. When these common targets were integrated into the Metascape database, the GO functional annotations, together with KEGG enrichment analyses, indicated that these targets were closely related to a variety of cancers and were involved in cell cycle signaling pathways. Protein–protein interaction (PPI) scrutiny of the cell cycle-centric targets pinpointed the profound association of GSK3β with the G2/M phase (Figure 6A). Further analysis of transcriptomic genes and network pharmacology targets revealed enrichment in the cell cycle, identifying GSK3β as a key upstream cell cycle regulator (Figure 6B).

Molecular Docking Combined with in vivo and in vitro Experiments Confirms GSK3β as the Key Target

From the PDBbind benchmark dataset, we selected the structural complex 1Q5K associated with GSK3β. From the literature, we identified AR-A014418 as a corresponding inhibitor. Docking studies revealed that the CDOCKER interaction energy between GSK3β (PDB: 1Q5K) and Alkannin was 38.3161 kcal/mol, whereas it was 37.4818 kcal/mol for AR-A014418 (Supplementary Table 1), indicating a strong binding interaction between Alkannin and GSK3β (Figure 7A). Immunohistochemistry showed that the expression of p-GSK3β was significantly decreased in the Alkannin group (Figure 7B). Western blot analysis confirmed this finding, revealing a dose-dependent reduction in GSK3β and p-GSK3β protein levels and increased WAF1/Cip1 (p21) expression after Alkannin treatment (Figure 7C). These findings suggest that Alkannin inhibits GSK3β and upregulates p21, leading to G2/M phase arrest in ESCC cells, which is consistent with prior results.

Alkannin Inhibits the Growth of BALB/c Nude Mouse Xenografts

To assess the in vivo antitumor properties of Alkannin, ESCC xenograft models were established in BALB/c-nu mice using KYSE150 cells (Figure 8A), followed by Alkannin treatment (saline control, 2 mg/kg, 4 mg/kg). The results showed that Alkannin treatment significantly slowed xenograft tumor growth (Figure 8B and C) and reduced tumor weight (Figure 8D). H&E staining indicated reduced cell numbers and nuclear abnormalities (condensation and fragmentation) in tumor tissues following Alkannin treatment. Immunohistochemical staining for Ki67 revealed a decrease in Ki67-positive cells in samples treated with Alkannin (Figure 8E), confirming suppressed tumor proliferation. These findings collectively demonstrate that Alkannin effectively inhibits the growth of xenograft tumors in nude mice.

Discussion

Surgical resection combined with adjuvant radiotherapy and chemotherapy is currently the primary treatment method for esophageal cancer.[22,23] However, postoperative local recurrence and metastasis pose significant challenges to treatment in clinical practice. Targeted drug therapies focus on specific molecular mechanisms in cancer cells, inhibiting tumor growth, spread, and blood supply while minimizing impact on normal cells. These therapies offer advantages such as personalized treatment, high efficacy, and fewer side effects.[24,25] Consequently, exploring new targeted anticancer drugs is crucial in the treatment of ESCC. In this study, we found that Alkannin significantly inhibited the growth of ESCC cells both in vivo and in vitro. This effect may be achieved by suppressing the expression of GSK3β, which causes G2/M phase cell cycle arrest, thereby inhibiting migration and invasion and inducing cell apoptosis.

A primary characteristic of tumor cells is their uncontrolled proliferation caused by an abnormal cell cycle, which endows tumor cells with invasive, metastatic, and antiapoptotic properties.[26] In this study, we noted a reduction in both ESCC cell viability and colony formation, along with a decrease in PCNA expression, following Alkannin treatment. These observations indicate that Alkannin significantly inhibits the proliferation of ESCC cells (Figure 1). The cell cycle consists of G1, S, G2, and M phases. Targeting the G2/M checkpoint has been shown to enhance radiotherapy efficacy and control tumor growth.[27] Arresting cells in the G2/M phase can reduce HeLa cell migration and invasion,

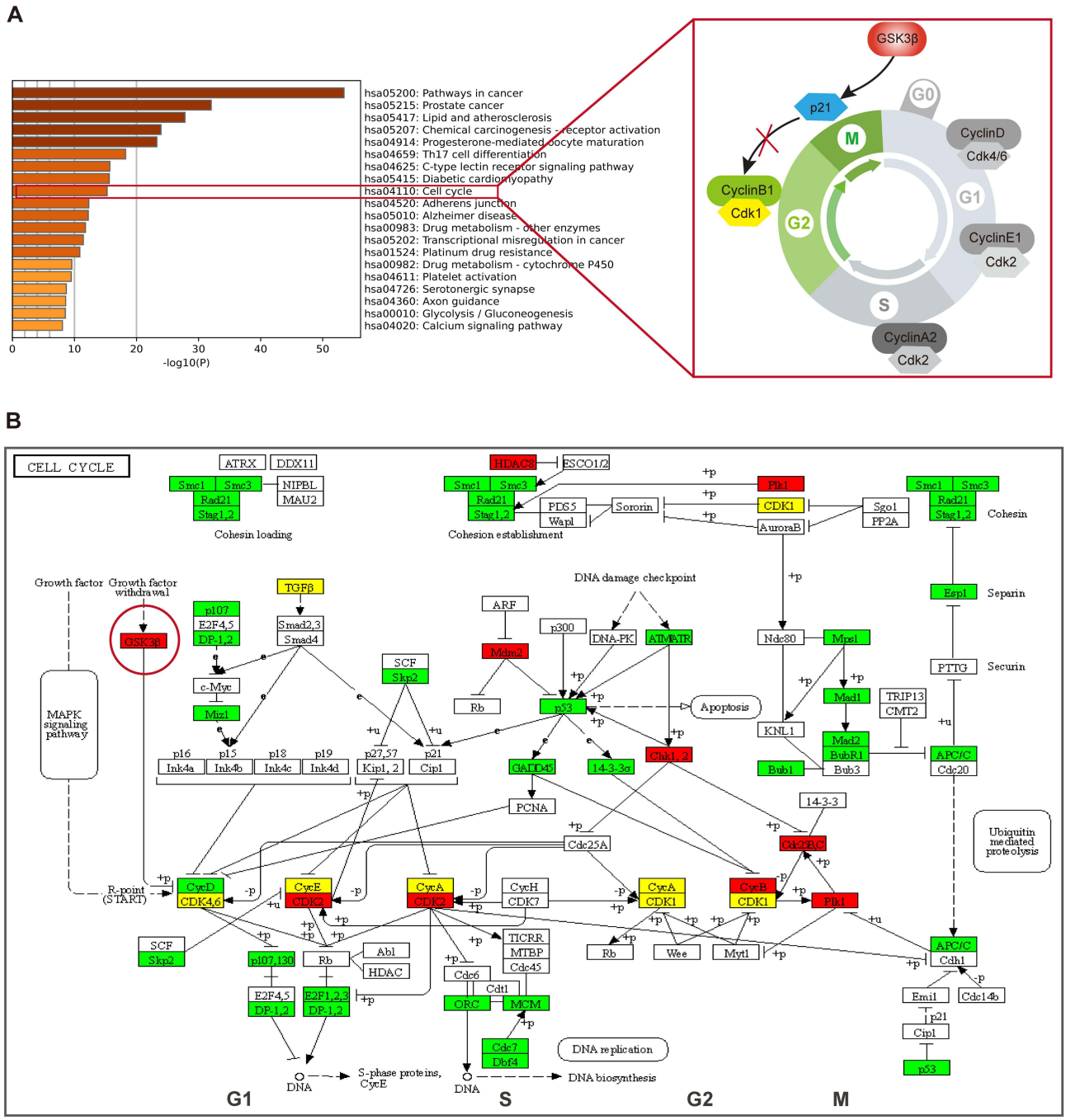

Figure 6 Network pharmacology and transcriptomics predict GSK3β as a key G2/M phase regulator. **(A)** Protein-protein interaction (PPI) network analysis shows GSK3β is closely associated with the G2/M phase related targets. **(B)** Transcriptomic and network pharmacology analyses show GSK3β is the key upstream regulator of the cell cycle. Red labels: network pharmacology targets; Green labels: transcriptome related differential genes; Yellow labels: both involved in.

demonstrating antitumor effects.[28] Recent findings indicate that modulating E-cadherin gene expression during the G2/M phase is more effective at inhibiting tumor invasion and metastasis than modulating E-cadherin gene expression during the G1 and S phases.[29] In this study, we found that Alkannin effectively inhibited the migration and invasion of ESCC cells and induced G2/M phase arrest in these cells (Figures 2–4). Moreover, G2/M phase arrest is linked to apoptosis. Qian et al reported that modulating this phase reduces the mitochondrial potential, promoting apoptosis in nasopharyngeal carcinoma cells. Similarly, allicin treatment led to G2/M arrest and apoptosis in skin cancer cells.[30,31] In our study, Annexin V-FITC/PI staining and Bax/Bcl-2 expression analysis showed that Alkannin induces apoptosis in ESCC

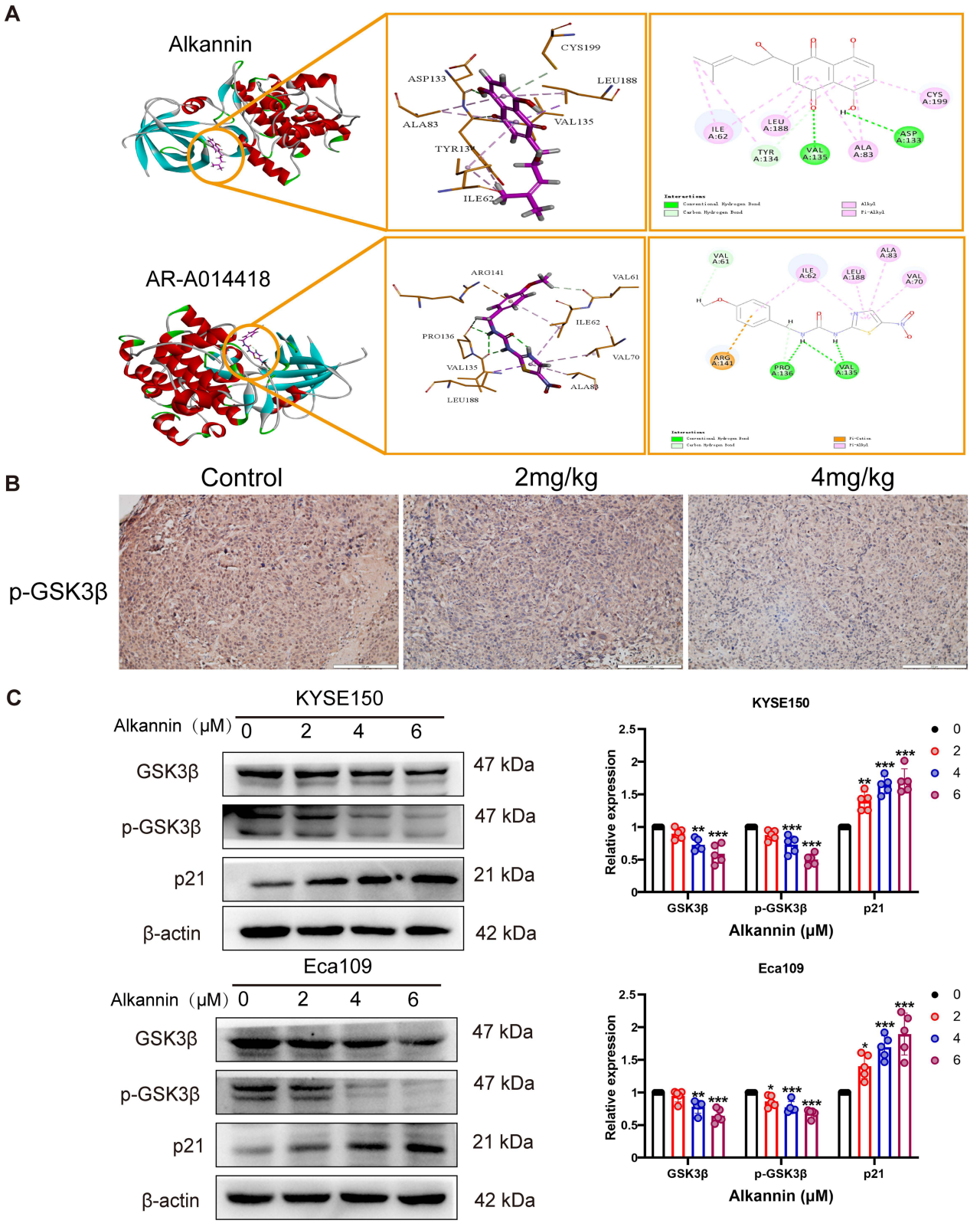

Figure 7 Alkannin has anti-ESCC effect via targeting GSK3β. **(A)** Molecular docking of Alkannin with GSK3β. **(B)** Immunohistochemistry analyzes the protein levels of p-GSK3β in xenograft tumor tissues. **(C)** Western blot analyzes the protein levels of GSK3β, p-GSK3β, and p21 in KYSE150 and Eca109 cells treated with Alkannin. Data are expressed as means ± SD from five independent experiments, **P* < 0.05; ***P* < 0.01; ****P* < 0.001 compared to control by one-way ANOVA.

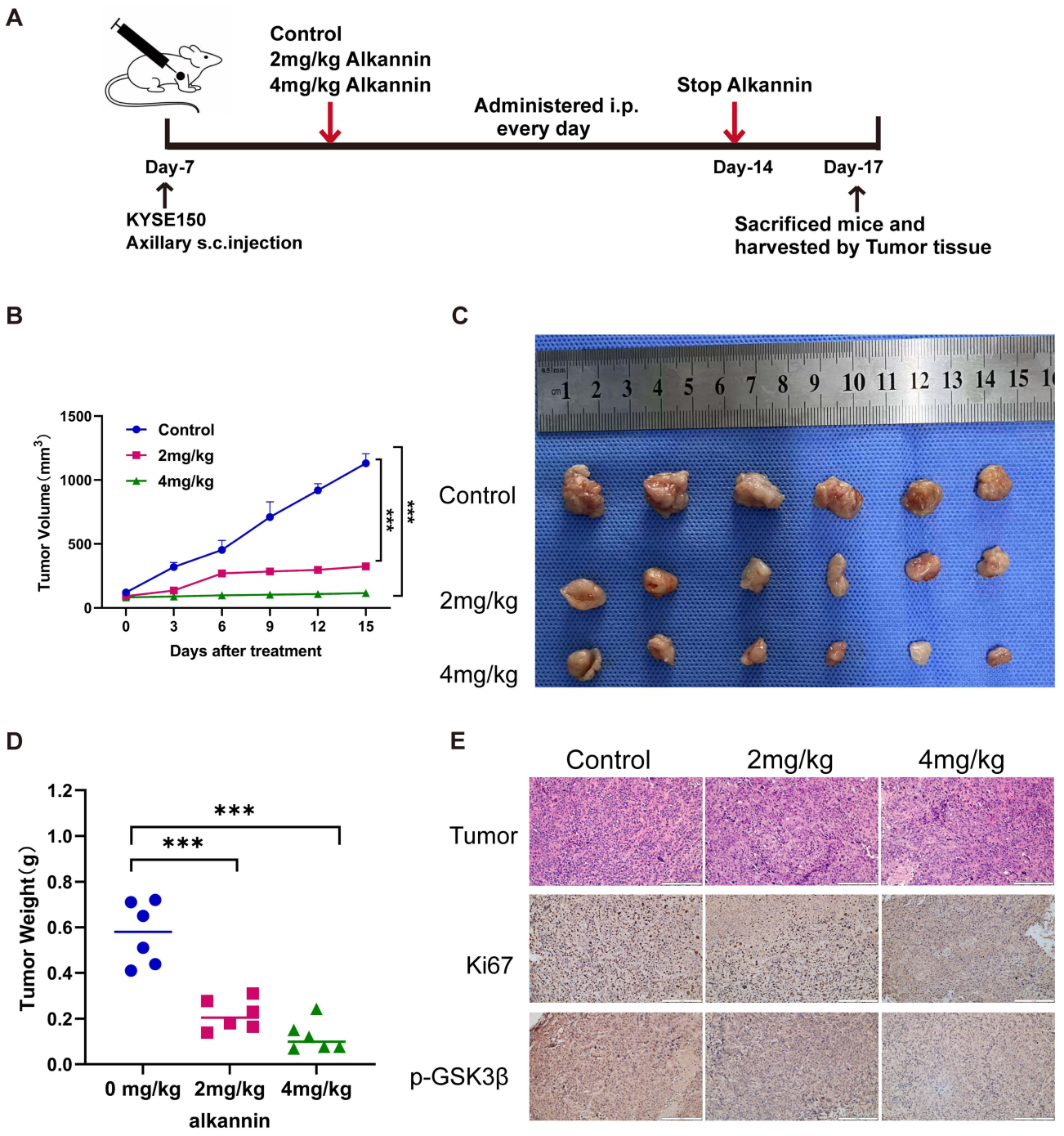

Figure 8 Alkannin inhibits the growth of ESCC xenograft tumors. **(A)** The flowchart of the ESCC xenograft tumor establishment and Alkannin intervention. **(B)** The changes of the tumor volume after treatment with Alkannin. **(C)** Representative images of tumors in different groups (n = 6). **(D)** The weight of xenograft tumors in different groups. **(E)** HE staining and immunohistochemistry analyzes the Ki67 and p-GSK3β protein expression. Data are expressed as means ± SD from six independent experiments, ***$P < 0.001$ compared to control by one-way ANOVA.

cells (Figures 3 and 4). Interestingly, Shikonin a typical isomer of Alkannin derived from *Lithospermum erythrorhizon*, induces G0/G1 phase arrest in Eca109 and EC9706 cells, thereby affecting the cell cycle proliferation process.[32] In contrast, our research indicated that Alkannin inhibits the migration and invasion and induces the apoptosis of ESCC cells by inducing G2/M phase arrest, demonstrating a mechanism distinct from that of Shikonin. This finding suggests for the first time that Alkannin exerts its antitumor effects by influencing cell cycle progression.

To further investigate the molecular mechanisms of Alkannin in ESCC, transcriptomic sequencing analysis of KYSE150 cells identified 4587 significantly differentially expressed genes (DEGs), with 2534 upregulated and 2053 downregulated (Figure 5A and 5B). Additionally, our exploration of potential Alkannin targets in ESCC treatment using network pharmacology identified 239 common targets.

Interestingly, our findings revealed that Alkannin's main anticancer pathway is linked to the cell cycle signaling pathway, which specifically involves G2/M cell cycle arrest, as demonstrated by KEGG and GO enrichment analyses from transcriptomic sequencing and network pharmacology (Figure 5C–E). Additionally, we confirmed that GSK3β serves as a core and upstream regulator in the cell cycle process and was identified as a key target in Alkannin's anti-ESCC effects through degree value calculations (Figure 6). Moreover, the results of molecular docking demonstrated Alkannin had stronger binding affinities for GSK3β than the other inhibitors (Figure 7A). This finding suggested that Alkannin may exert its anti-ESCC effect by modulating the cell cycle process and targeting GSK3β.

GSK3β is a serine/threonine kinase that phosphorylates glycogen synthase, not only elevates the body's blood glucose levels but also plays a role in combating cancer by participating in tumor cell cycle progression.[33] Cao et al reported that inhibition of GSK3β suppresses the proliferation and survival of human ovarian cancer cells, while high expression of GSK3β facilitates entry into the S phase and increases cyclin D1 expression, thereby accelerating the migration and invasion of ovarian cancer cells.[34] Menschikowski et al discovered that treating cancer cells with GSK3β inhibitors reduces DNA replication, which causes cell cycle arrest at the S phase and decreases the expression of cyclin A and cyclin E, thereby inducing apoptosis.[35] Recent studies have shown that GSK3β expression is significantly greater in esophageal cancer tissues than in normal esophageal epithelial tissues.[36] Inhibiting GSK3β reduces CyclinB1 levels and induces G2/M phase arrest in the Eca109 cell line.[37] In our study, the inhibition of GSK3β by Alkannin led to G2/M phase arrest and reduced the expression of Cyclin B1 and CDK1, thus inhibiting the migration and invasion of ESCC cells and inducing apoptosis. During the cell cycle, p21 blocks CDK1/CyclinB1 activation, leading to G2/M phase arrest and antitumor effects.[38] Previous studies have shown that GSK3β inhibition in colorectal cancer increases p21 levels, reduces Cyclin B1 and cdc2 expression, and leads to G2/M phase arrest and apoptosis.[39] In contrast, GSK3β upregulation in pancreatic cancer activates Cyclin D1, suppresses p21, and drives cancer progression.[40] Our study revealed that Alkannin treatment of ESCC cells resulted in increased p21 expression and decreased Cyclin B1 and CDK1 expression. These findings indicate that Alkannin can upregulate p21 protein levels through GSK3β, leading to the arrest of ESCC cells in the G2/M phase. Notably, shikonin inhibits aerobic glycolysis by targeting PKM2[41] and regulates the proliferation, migration, and invasion of esophageal cancer cells through the phosphorylation of STAT3 in the TGF-β1-induced EMT pathway.[2] Our study showed that Alkannin may inhibit the expression of GSK3β, causing G2/M phase arrest in ESCC cells and thereby inhibiting migration and invasion and inducing the apoptosis of ESCC cells. This suggests that both Shikonin and Alkannin, despite originating from the same plant, *Lithospermum erythrorhizon*, have anti-ESCC effects through different mechanisms. Our research demonstrated the potential of Alkannin as a therapeutic agent for ESCC treatment, particularly as a GSK3β targeting drug. Future studies will focus on GSK3β inhibition and gene knockout techniques to more precisely determine the anticancer mechanisms of GSK3β. Furthermore, we also confirmed that Alkannin significantly inhibits tumor growth in a concentration-dependent manner in a xenograft mouse model. Importantly, Alkannin significantly decreased the protein expression of p-GSK3β compared to the model group (Figure 7B and C).

GSK3β is involved in several tumor-related signaling pathways. The inhibition of GSK3β can block NF-κB nuclear translocation, reducing pro-inflammatory factor expression and slowing tumor progression.[42] Additionally, in the Hedgehog-Gli pathway, GSK3β inhibition reduces cancer cell proliferation and induces apoptosis,[43] while in the TGFβ/Smad pathway, it mitigates the invasive phenotype driven by sFRP1.[44] Therefore, GSK3β serves as a promising therapeutic target. These studies further inspire us to explore the possible signal pathway mediated by GSK3β in the Alkannin anti-ESCC effect in the future. Some promising therapeutic anticancer compounds showed available anticancer effects and were found to inhibit GSK3β with low toxicity.[45] It is reported that Alkannin shows relatively low toxicity to H9c2 cells.[46] These studies indicate that Alkannin might be a potential anticancer drug with low toxicity by targeting GSK3β.

Conclusion

In the study, Alkannin significantly inhibited tumor growth in a concentration-dependent manner, accompanied by the reduction in Ki67 and p-GSK3β protein expression in a xenograft mouse model. Furthermore, Alkannin induced G2/M phase arrest and apoptosis, and inhibited migration and invasion in ESCC cell lines KYSE150 and Eca109, which exhibited inhibited expression of p-GSK3β protein. These results preliminarily indicated that Alkannin has a prominent anti-ESCC effect, which might be through targeting GSK3β both in vivo and in vitro. This study preliminarily demonstrates that Alkannin might be a potential GSK3β-targeting anticancer drug, which could provide a new natural anticancer compound as a candidate drug and offer new therapeutic strategies for clinical use.

Data Sharing Statement

The data will be made available upon request from the corresponding author, Ketao Ma.

Ethics Statement

This animal experiment was reviewed and approved by the Bioethics Committee of Shihezi University (A2024-193). All experiments were conducted under the "Guidelines for the Care and Use of Laboratory Animals" set by the National Institute for Health of China.

Acknowledgments

We are grateful to the Key Laboratory of Xinjiang Endemic and Ethnic Diseases, NHC Key Laboratory of Prevention and Treatment of Central Asia High Incidence Diseases, and the Department of Physiology and Pathophysiology of Shihezi University School of Medicine.

Funding

National Natural Science Foundation of China, Grant/Award Number: 82260492; Training Program of Tianshan Talents (to Ketao Ma and Xinzhi Li); Guiding Project of Xinjiang Production and Construction Corps, Grant/Award Number: 2022ZD042; Youth Innovation and Talent Cultivation Program of Shihezi University; Grant/Award Number: CXPY202217; High Level of Scientific Research Project of Shihezi University, Grant/Award Number: RCZK202030; High Level of Scientific Research Project of Shihezi University, Grant/Award Number: RCZK2021B27; Technical Innovation Talent Planning, Grant/Award Number: 2023CB008-07.

Disclosure

The authors declare that the research was conducted in the absence of any commercial or financial relationships that could be construed as potential conflict of interest.

References

1. Sung H, Ferlay J, Siegel RL, et al. Global cancer statistics 2020: globocan estimates of incidence and mortality worldwide for 36 cancers in 185 countries. *CA Cancer J Clin*. 2021;71(3):209–249. doi:10.3322/caac.21660
2. Ma R, Liu Q, Zheng S, et al. Pkm2-regulated stat3 promotes esophageal squamous cell carcinoma progression via tgf-β1-induced emt. *J Cell Biochem*. 2019;120(7):11539–11550. doi:10.1002/jcb.28434
3. Chen R, Zheng R, Zhang S, et al. Patterns and trends in esophageal cancer incidence and mortality in China: an analysis based on cancer registry data. *J Natl Cancer Cent*. 2023;3(1):21–27. doi:10.1016/j.jncc.2023.01.002
4. Abnet CC, Arnold M, Wei W-Q. Epidemiology of esophageal squamous cell carcinoma. *Gastroenterology*. 2018;154(2):360–373. doi:10.1053/j.gastro.2017.08.023
5. Yang H, Liu H, Chen Y, et al. Neoadjuvant chemoradiotherapy followed by surgery versus surgery alone for locally advanced squamous cell carcinoma of the esophagus (neocrtec5010): a Phase III multicenter, randomized, open-label clinical trial. *J Clin Oncol*. 2018;36(27):2796–2803. doi:10.1200/jco.2018.79.1483
6. Bang Y-J, Van Cutsem E, Feyereislova A, et al. Trastuzumab in combination with chemotherapy versus chemotherapy alone for treatment of her2-positive advanced gastric or gastro-oesophageal junction cancer (toga): a Phase 3, open-label, randomised controlled trial. *Lancet*. 2010;376(9742):687–697. doi:10.1016/s0140-6736(10)61121-x
7. Walz AL, Ugolkov A, Chandra S, et al. Molecular pathways: revisiting glycogen synthase kinase-3β as a target for the treatment of cancer. *Clin Cancer Res*. 2017;23(8):1891–1897. doi:10.1158/1078-0432.Ccr-15-2240

8. Domoto T, Uehara M, Bolidong D, et al. Glycogen synthase kinase 3β in cancer biology and treatment. *Cells*. 2020;9(6):1388. doi:10.3390/cells9061388
9. Yoshino Y, Ishioka C. Inhibition of glycogen synthase kinase-3 beta induces apoptosis and mitotic catastrophe by disrupting centrosome regulation in cancer cells. *Sci Rep*. 2015;5(1):13249. doi:10.1038/srep13249
10. Chikano Y, Domoto T, Furuta T, et al. Glycogen synthase kinase 3β sustains invasion of glioblastoma via the focal adhesion kinase, rac1, and c-jun n-terminal kinase-mediated pathway. *Mol Cancer Ther*. 2015;14(2):564–574. doi:10.1158/1535-7163.Mct-14-0479
11. Kitano A, Shimasaki T, Chikano Y, et al. Aberrant glycogen synthase kinase 3β is involved in pancreatic cancer cell invasion and resistance to therapy. *PLoS One*. 2013;8(2):e55289. doi:10.1371/journal.pone.0055289
12. Bolidong D, Domoto T, Uehara M, et al. Potential therapeutic effect of targeting glycogen synthase kinase 3β in esophageal squamous cell carcinoma. *Sci Rep*. 2020;10(1):11807. doi:10.1038/s41598-020-68713-9
13. Kaur K, Sharma R, Singh A, et al. Pharmacological and analytical aspects of alkannin/shikonin and their derivatives: an update from 2008 to 2022. *Chin Herb Med*. 2022;14(4):511–527. doi:10.1016/j.chmed.2022.08.001
14. Zhang Z, Wen C, Jia M, Zhang H, Sun S-Q. Alkannin exerts antitumor properties in cutaneous squamous cell carcinoma by inducing apoptosis and shifting the m1/m2 polarization of tumor-associated macrophages by upregulating PTEN. *Kaohsiung J Med Sci*. 2023;39(1):70–79. doi:10.1002/kjm2.12617
15. Mao Y, Zhang W, Zhang R, Zuo J. Alkannin restrains oral squamous carcinoma cell growth, migration and invasion by regulating microRNA-9/reck axis. *Artif Cells Nanomed Biotechnol*. 2019;47(1):3153–3162. doi:10.1080/21691401.2019.1642206
16. Vinitha R, Revanasiddappa BC, Mahendra GS, et al. Cytotoxic and apoptotic efficacy of alkanna tinctoria on glioma cells. *Nat Prod Res*. 2022;37(22):3873–3877. doi:10.1080/14786419.2022.2155644
17. Gao C, Liang C, Nie Z, Liu Y, Wang J, Zhang D. Alkannin inhibits growth and invasion of glioma cells c6 through iqgap/mtor signal pathway. *Int J Clin Exp Med*. 2015;8(4):5287–5294.
18. Trinath D, Rishika P, Suneetha Y. In silico screening and identification of potential gsk3β inhibitors. *J Recept Signal Transd Res*. 2018;38(4):279–289. doi:10.1080/10799893.2018.1478854
19. Ratan VB, Yafeng X, Stefan von B, et al. Structural insights and biological effects of glycogen synthase kinase 3-specific inhibitor ar-a014418. *J Biol Chem*. 2003;278(46):45937–45945. doi:10.1074/jbc.m306268200
20. Hu H, Xu W, Zhang W-X, et al. Identification of mir-515-3p and its targets, vimentin and mmp3, as a key regulatory mechanism in esophageal cancer metastasis: functional and clinical significance. *Signal Transduct Target Ther*. 2020;5(1):271. doi:10.1038/s41392-020-00275-8
21. Nakamura N, Fujihara H, Kawaguchi K, et al. Possible action of olaparib for preventing invasion of oral squamous cell carcinoma in vitro and in vivo. *Int J Mol Sci*. 2022;23(5). doi:10.3390/ijms23052527
22. Harada K, Rogers JE, Iwatsuki M, Yamashita K, Baba H, Ajani JA. Recent advances in treating oesophageal cancer. *F1000Res*. 2020;9. doi:10.12688/f1000research.22926.1
23. Lagergren J, Smyth E, Cunningham D, Lagergren P. Oesophageal cancer. *Lancet*. 2017;390(10110):2383–2396. doi:10.1016/s0140-6736(17)31462-9
24. Yang H, Li X, Yang W. Advances in targeted therapy and immunotherapy for esophageal cancer. *Chin Med J*. 2023;136(16):1910–1922. doi:10.1097/cm9.0000000000002768
25. Ying J, Zhang M, Qiu X, Yu L. The potential of herb medicines in the treatment of esophageal cancer. *Biomed Pharmacother*. 2018;103:381–390. doi:10.1016/j.biopha.2018.04.088
26. Liu K, Zheng M, Lu R, et al. The role of cdc25c in cell cycle regulation and clinical cancer therapy: a systematic review. *Cancer Cell Int*. 2020;20:213. doi:10.1186/s12935-020-01304-w
27. Dillon MT, Good J, Harrington KJ. Selective targeting of the g2/m cell cycle checkpoint to improve the therapeutic index of radiotherapy. *Clin Oncol*. 2014;26(5):257–265. doi:10.1016/j.clon.2014.01.009
28. Cao J, Wu Q, Zheng W, Li L, Mei W. Correction: microwave-assisted synthesis of polypyridyl ruthenium(ii) complexes as potential tumor-targeting inhibitors against the migration and invasion of hela cells through g2/m phase arrest. *RSC Adv*. 2020;10(52):31525. doi:10.1039/d0ra90091e
29. Xie L, Wang J, Song L, Jiang T, Yan F. Cell-cycle dependent nuclear gene delivery enhances the effects of e-cadherin against tumor invasion and metastasis. *Signal Transduct Target Ther*. 2023;8(1):182. doi:10.1038/s41392-023-01398-4
30. Qian D, Zheng W, Chen C, Jing G, Jun-xuan H. Roles of ccnb2 and nkx3-1 in nasopharyngeal carcinoma. *Cancer Biother Radiopharm*. 2020;35(3):208–213. doi:10.1089/cbr.2019.3016
31. Wang HC, Yang JH, Hsieh S-C, Sheen LY. Allyl sulfides inhibit cell growth of skin cancer cells through induction of DNA damage mediated g2/m arrest and apoptosis. *J Agric Food Chem*. 2010;58(11):7096–7103. doi:10.1021/jf100613x
32. Tang J-C, Zhao J, Long F, et al. Efficacy of shikonin against esophageal cancer cells and its possible mechanisms in vitro and in vivo. *J Cancer*. 2018;9(1):32–40. doi:10.7150/jca.21224
33. Pizarro J, Folch J, Esparza JL, Jordan J, Pallás M, Camins A. A molecular study of pathways involved in the inhibition of cell proliferation in neuroblastoma b65 cells by the gsk-3 inhibitors lithium and sb-415286. *J Cell Mol Med*. 2009;13(9B):3906–3917. doi:10.1111/j.1582-4934.2008.00389.x
34. Cao Q, Lu X, Feng Y. Glycogen synthase kinase-3beta positively regulates the proliferation of human ovarian cancer cells. *Cell Res*. 2006;16(7):671–677. doi:10.1038/sj.cr.7310078
35. Menschikowski M, Hagelgans A, Tiebel O, et al. Regulation of thrombomodulin expression in prostate cancer cells. *Cancer Lett*. 2012;322(2):177–184. doi:10.1016/j.canlet.2012.03.001
36. Kang L, Liu Y, He J, et al. Gsk3β-driven sox2 overexpression is a targetable vulnerability in esophageal squamous cell carcinoma. *Oncogene*. 2023;42(30):2297–2314. doi:10.1038/s41388-023-02748-w
37. Wang J, Wang C-L, Wen J, Wang Y, Hu Y-B, Ren H. Lithium inhibits proliferation of human esophageal cancer cell line eca-109 by inducing a g2/m cell cycle arrest. *World J Gastroenterol*. 2008;14(25):3982–3989. doi:10.3748/wjg.14.3982
38. Wu K, Chi C, Lai JCY, Chen Y-J, Kou YR. Tlc388 induces DNA damage and g2 phase cell cycle arrest in human non-small cell lung cancer cells. *Cancer Control*. 2020;27(1):1073274819897975. doi:10.1177/1073274819897975
39. Dewi FRP, Domoto T, Hazawa M, et al. Colorectal cancer cells require glycogen synthase kinase-3β for sustaining mitosis via translocated promoter region (tpr)-dynein interaction. *Oncotarget*. 2018;9(17):13337–13352. doi:10.18632/oncotarget.24344

40. Ma S, Li Q, Pan F. Cxcr4 promotes gsk3β expression in pancreatic cancer cells via the akt pathway. *Int J Clin Oncol*. 2014;20(3):525–530. doi:10.1007/s10147-014-0740-0
41. Zhang Q, Liu Q, Zheng S, et al. Shikonin inhibits tumor growth of ESCC by suppressing pkm2 mediated aerobic glycolysis and stat3 phosphorylation. *J Cancer*. 2021;12(16):4830–4840. doi:10.7150/jca.58494
42. Saud SM, Li W, Gray Z, et al. Diallyl disulfide (dads), a constituent of garlic, inactivates nf-κb and prevents colitis-induced colorectal cancer by inhibiting gsk-3β. *Cancer Prev Res*. 2016;9(7):607–615. doi:10.1158/1940-6207.CAPR-16-0044
43. Trnski D, Sabol M, Gojević A, et al. Gsk3β and gli3 play a role in activation of hedgehog-gli pathway in human colon cancer - targeting gsk3β downregulates the signaling pathway and reduces cell proliferation. *Biochim Biophys Acta*. 2015;1852(12):2574–2584. doi:10.1016/j.bbadis.2015.09.005
44. Peng J-X, Liang S-Y, Li L. Sfrp1 exerts effects on gastric cancer cells through gsk3β/rac1-mediated restraint of tgfβ/smad3 signaling. *Oncol Rep*. 2019;41(1):224–234. doi:10.3892/or.2018.6838
45. Libo H, Farah A, Alaa S, et al. Identifying promising gsk3β inhibitors for cancer management: a computational pipeline combining virtual screening and molecular dynamics simulations. *Front Chem*. 2023; 11:1200490. doi:10.3389/fchem.2023.1200490
46. Nadire Ö, Neslihan SÖN, Merve Yüzbaşıoğlu B, et al. Structure-activity relationship of anticancer drug candidate quinones. *Turk J Chem*. 2024;48(1):152–165. doi:10.55730/1300-0527.3647